



Power-law and log-normal avalanche size statistics in random growth processesStefano Polizzi ^{1,2}, Francisco-José Pérez-Reche,³ Alain Arneodo,² and Françoise Argoul ^{2,*}¹*Ecole Normale Supérieure de Lyon, 69342 Lyon, France*²*Université Bordeaux, CNRS, LOMA, UMR 5798, F-33405 Talence, France*³*Institute for Complex Systems and Mathematical Biology, SUPA, University of Aberdeen, AB24 3UE, United Kingdom*

(Received 25 June 2021; accepted 14 October 2021; published 8 November 2021)

We study the avalanche statistics observed in a minimal random growth model. The growth is governed by a reproduction rate obeying a probability distribution with finite mean \bar{a} and variance v_a . These two control parameters determine if the avalanche size tends to a stationary distribution (*finite scale* statistics with finite mean and variance, or *power-law* tailed statistics with exponent $\in (1, 3)$), or instead to a nonstationary regime with *log-normal* statistics. Numerical results and their statistical analysis are presented for a uniformly distributed growth rate, which are corroborated and generalized by mathematical results. The latter show that the numerically observed avalanche regimes exist for a wide family of growth rate distributions, and they provide a precise definition of the boundaries between the three regimes.

DOI: [10.1103/PhysRevE.104.L052101](https://doi.org/10.1103/PhysRevE.104.L052101)

In complex systems with long-range spatiotemporal correlations, avalanche processes are commonly observed. Well-known examples of avalanches include the spreading of epidemics (or information) [1,2], the price evolution of stock options in finance [3], avalanches of neuron firings in the brain [4–6], “crackling noise” exhibited by earthquakes [7,8], structural phase transitions [9,10] and magnetic systems [11,12], or avalanches of fractures in porous media [13] or living systems [14,15]. A crucial quantity to characterize avalanches is their size distribution, which allows theoretical and experimental results to be compared and can suggest mechanisms for the underlying avalanche dynamics. Notably, heavy-tailed distributions are often observed for avalanche size statistics, and understanding them is important to determine the origin of the specific process. From a practical viewpoint, it is often difficult to distinguish the type of heavy-tailed distributions on finite intervals, especially for limited size samples or noisy data. Pareto (power-law) and log-normal distributions are two of the most widely observed heavy-tailed distributions [16,17]. Many investigations have described heavy-tailed data in terms of Pareto or power laws with exponential decays [18]. Careful statistical analyses, however, indicated that statistical evidence in support of a power-law distribution is often limited [19], and a log-normal distribution can often be a good alternative to describe heavy-tailed statistics [20]. These difficulties are clearly exemplified by the ongoing controversy between log-normal and power-law distributions in neuroscience [21,22] and complex networks [23]. The discrimination between power-law and log-normal distributions is even more challenging for data that can be modeled as a log-normal distribution at moderate sizes with a power-law tail [24].

Several paradigmatic models have been proposed to explain the ubiquity of power-law avalanche size distributions. These include critical points in disordered systems [11,25–28], self-organized criticality (SOC) [29], marginal stability [30], and, in more abstract terms, growth models [31] or branching processes [32–35]. In fact, some of these paradigms are related, or can even be mapped, to each other (e.g., SOC and branching processes [36] or branching processes and spin models [37]).

Log-normal distributions are often explained in terms of stochastic multiplicative models of growth phenomena based on the law of proportionate effect. Here, we focus on Gibrat’s process [38,39], which can be viewed as a discrete time version of the so-called multiplicative noise [40]. Gibrat’s process assumes that the size z_i of an observable in generation i grows proportionally to its size with a random reproduction (or growth) rate, a_i : $z_{i+1} = a_i z_i$. Assuming that the growth rates $\{a_i\}_{i=1}^{\infty}$ are independent random variables and the first two moments of $\ln a_i$ are finite for every i , the central limit theorem implies that z_i is log-normally distributed for large i [17], or see [41] for a more precise approximation. Avalanches are typically regarded as bursts of activity, which in our case would correspond to excursions of z that asymptotically return to the absorbing state with $z = 0$ after being perturbed from this state. Since Gibrat’s variable z can either approach zero or ∞ when iterated, we extend the usual avalanche definition to encompass the case in which z does not return to 0 but grows indefinitely, as in supercritical branching processes [32]. The size of an avalanche corresponds to the sum of z_i over generations. Despite the fact that the distribution of z_i is reasonably well understood for Gibrat’s processes, little is known about the avalanche size distribution. In general, a log-normal distribution for z_i does not imply a log-normal distribution for the avalanche size, and Gibrat’s process cannot be regarded as an explanation of log-normal avalanche size statistics.

*francoise.argoul@u-bordeaux.fr

Here, we push further the comparative analysis between power-law and log-normal distributions by studying the avalanche size distribution of Gibrat's processes. By means of mathematical results and numerical simulation examples, we reveal rich avalanche behavior, which, in particular, includes power-law and log-normal avalanche size statistics.

The model. The basis of our avalanche model is the following multiplicative process:

$$z_{i+1} = a_i z_i = a_i z_0 \prod_{j=0}^{i-1} a_j. \quad (1)$$

The initial value z_0 for the process represents a perturbation of the system from the $z = 0$ absorbing state. We set $z_0 = 1$ (a different positive value of z_0 would only lead to a time shift). The reproduction rates $\{a_n\}_{n=0}^{\infty}$ are independent and identically distributed (i.i.d.) random variables with finite mean $\bar{a} = \mathbb{E}_a[a]$ and variance $v_a = \mathbb{E}_a[a^2] - \mathbb{E}_a^2[a]$. In our model, the probability density function (PDF) for the reproduction rate, $f_a(a)$, is required to have a non-negative support to ensure that $z_i \geq 0$ at every generation i .

The avalanche size after T generations is given by the following sum:

$$Z_T = \sum_{i=1}^T z_i = a_1 + a_1 a_2 + \dots + a_1 \dots a_T. \quad (2)$$

Our aim is to understand the dependence of the PDF for the avalanche size, $p(Z_T)$, on the two parameters of the reproduction rate distribution, \bar{a} and v_a . Equation (2) shows that the avalanche size Z_T is a random variable given by the sum of T random variables. The challenge in calculating $p(Z_T)$ is that $\{z_i\}_{i=1}^T$ are correlated, and the central limit theorem does not apply in general [42]. Accordingly, there is no reason to expect that Z_T is normally distributed for large T , as one would expect if $\{z_i\}_{i=1}^T$ were uncorrelated. In fact, Eq. (2) shows that Z_T is a Kesten scalar variable [43]. Within this context, power-law tails have been reported for $p(Z_T)$ under quite general conditions [43–46]. Here, we identify power-law decay as one of three generic behaviors for $p(Z_T)$. In addition, our analysis establishes a conceptual link between a Kesten recursion and the size of avalanches described as Gibrat's multiplicative process.

We first present results of numerical simulations for a specific PDF $f_a(a)$ that show the existence of three different regimes for $p(Z_T)$. After that, we mathematically demonstrate that the numerically observed avalanche regimes are expected for any $f_a(a)$ with finite first and second moments for a and $\ln a$.

Numerical results. Here, we present results for a uniformly distributed reproduction rate, $a_i \sim \mathcal{U}(b, c)$, with $0 \leq b < c$. The uniform distribution is a simple and flexible choice that allows the dependence of $p(Z_T)$ on \bar{a} and v_a to be systematically studied by independently tuning the parameters $\bar{a} = (b + c)/2$ and $v_a = (c - b)^2/12$. In [47], we present qualitatively similar results for exponentially (Fig. S2 of Sec. IV) and Poisson (Fig. S3 of Sec. V) distributed growth rates. In both cases, however, \bar{a} and v_a cannot be independently tuned.

Figure 1 shows three avalanche regimes identified for uniformly distributed a on the (\bar{a}, v_a) space. The region of the

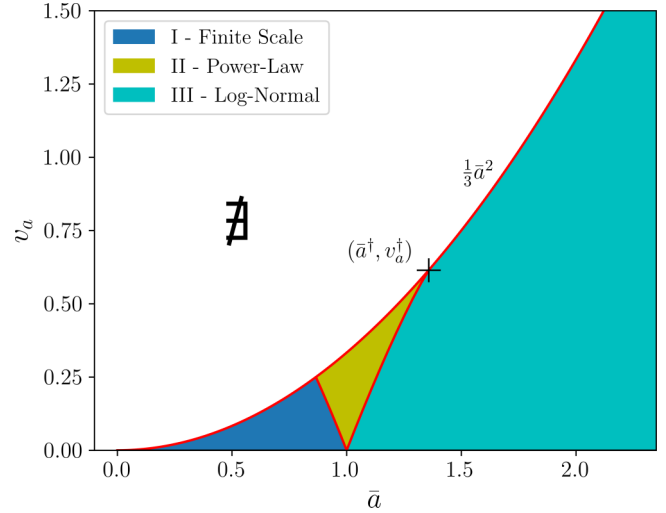


FIG. 1. Phase diagram on the (\bar{a}, v_a) space showing three regimes for the avalanche size distribution for uniformly distributed growth rate, $a \sim \mathcal{U}(b, c)$. In regime I (finite scale), $p(Z_T)$ converges to an asymptotic PDF $p(Z)$ with finite mean and variance. In regime II, $p(Z_T)$ converges to an asymptotic $p(Z)$ with a power-law tail. In regime III, Z_T is nonstationary and $p(Z_T)$ approaches a log-normal distribution for large T , with T -dependent parameters. All regimes are bounded from above by the condition $v_a \leq \bar{a}^2/3$ ensuring $b > 0$ and $(\bar{a}^\dagger \simeq 1.36, v_a^\dagger \simeq 0.61)$. Boundaries between different regimes were analytically obtained.

space where a random growth process is possible depends on the specific PDF for the growth rate. For uniformly distributed a , the region is restricted to $\bar{a} \geq 0$ and $v_a \in [0, \bar{a}^2/3]$. For a given \bar{a} , the upper bound for v_a reflects the constraint $b \geq 0$. For a general f_a , the upper bound is given by the condition $a \geq 0$.

Regime I (dark blue region in Fig. 1) is characterized by avalanches for which z_i approaches zero after a finite number of generations in such a way that the mean and variance of $p(Z_T)$ are finite for every T . This regime is referred to as the *finite scale* regime, as opposed to *scale-free* distributions, which lack a typical scale. Below, we mathematically show that the necessary condition for the first two moments of $p(Z_T)$ to be finite is $v_a + \bar{a}^2 < 1$ for any $f_a(a)$. In particular, this condition defines the boundary between regions I and II shown in Fig. 1 for a uniformly distributed a . In regime I, $p(Z_T)$ converges to an asymptotic PDF, $p(Z)$, after a finite number of generations, T_z . Figure 2(a) shows an example of the convergence of $p(Z_T)$ to $p(Z)$ after $T_z = 22$ generations. The rate of convergence decreases as the boundary with region II is approached. The specific shape of $p(Z)$ depends on \bar{a} and v_a . Phenomenologically, we observe that the subset of region I with $v_a \lesssim \bar{a} - 0.7$ (then excluding values of v_a just below the upper boundary) shows distributions that are compatible with a log-normal distribution [see Fig. 2(a)]. This result is reminiscent of cases in which a log-normal distribution was observed as the asymptotic distribution for the sum of a large but finite number of uncorrelated and log-normal, or, more generally, positively skewed random variables [48,49]. The comparison of our results with those in [48,49], however, is not complete due to the presence of correlations between the

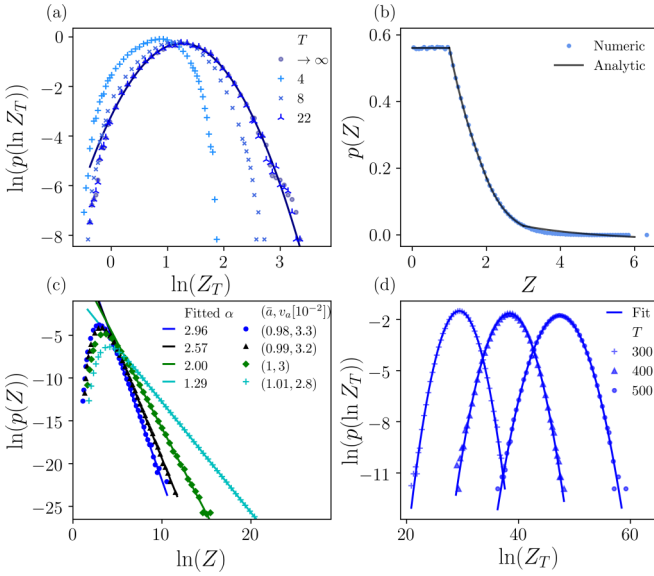


FIG. 2. Examples of avalanche size PDFs for a uniformly distributed growth rate, $a \sim \mathcal{U}(b, c)$. (a) Regime I: convergence of the PDF of $\ln Z_T$ toward an asymptotic distribution with T . $(\bar{a}, v_a) = (0.8, 0.06)$, solid line: fit of a log-normal distribution to the asymptotic distribution. (b) Asymptotic PDF $p(Z)$ for $(\bar{a}, v_a) = (0.5, \bar{a}^2/3)$ (i.e., $b = 0$ corresponding to the upper bound for v_a in Fig. 1). Solid line: analytical solution. (c) Regime II: asymptotic $p(Z)$ in log-log scale. Solid lines: fits of power laws with exponents α given in the legend. (d) Regime III: logarithm of $p(\ln Z_T)$ with $(\bar{a}, v_a) = (1.1, 0.013)$. Solid lines: fits of a log-normal distribution to the data for each given T . Symbols (respectively, solid lines) are used for numerical results (respectively, maximum-likelihood fits or analytical results).

random variables $\{z_i\}_{i=1}^T$, defining Z_T in our model. In fact, a log-normal-like distribution is observed in a good part of region I in the phase diagram, but it is not the only possible shape for $p(Z)$ in this regime. For instance, Fig. 2(b) shows an example of $p(Z)$ observed at a point along the upper bound for region I in the phase diagram (line with $v_a = \bar{a}^2/3$ in Fig. 1). See Sec. III A of [47] for more examples of $p(Z)$ in this regime.

In regime II, $p(Z_T)$ converges to an asymptotic PDF $p(Z)$ with a power-law (or Pareto) tail $Z^{-\alpha}$ [see Fig. 2(c)]. A maximum-likelihood fit to the data (Sec. VI of [47]) reveals that the exponent α takes values that range from $\alpha = 3$ at the boundary with regime I to $\alpha = 1$ at boundary with regime III. Below we mathematically show that this range for α holds beyond the uniformly distributed a used for the simulations shown in Fig. 2.

In regime III, avalanches grow indefinitely and $p(Z_T)$ does not converge to a T -independent PDF. Instead, the location and spread of $p(Z_T)$ increase monotonically with T [Fig. 2(d)]. Interestingly, $p(Z_T)$ can be very well described by a log-normal distribution with T -dependent parameters. This is corroborated by a likelihood ratio test [50] and parametric bootstrap [51] (see more details in Sec. VI of [47]).

Mathematical results. We now show mathematically that the three avalanche regimes illustrated numerically for uniformly distributed $\{a_i\}$ can be observed for generic

distributions $f_a(a)$ with non-negative support and finite first and second moments for a and $\ln a$. This analysis also provides general conditions satisfied at the boundaries between different regimes.

To study the PDF of the avalanche size Z_T for a generic $f_a(a)$, we express Eq. (2) as $Z_T = a_1(1 + X_T)$. Here, $X_T = \sum_{i=2}^T \prod_{j=2}^i a_j$ is a random variable whose behavior at large T determines whether the system is in regime I, II, or III. Regime III corresponds to situations in which $z_{T+1}/a_1 = \prod_{j=2}^T a_j$ increases monotonically with T . In this case, an infinite avalanche occurs in which z grows indefinitely and Z_T obeys a nonstationary log-normal distribution for large T , provided $\mathbb{E}_a[\ln^2 a] < \infty$. Indeed, in this case X_T is distributed as Z_{T-1} and therefore $Z_T \sim a_1 Z_{T-1}$ for large T . We then conclude that Z_T is given by the product of T i.i.d. positive random variables obeying $f_a(a)$ and, provided $\mathbb{E}_a[\ln^2 a] < \infty$, Z_T obeys a log-normal distribution with expectation and variance that increase exponentially with T (see the expressions for $\mathbb{E}[Z_T]$ and $\text{var}[Z_T]$ in Sec. II of [47]). In other words, Z_T essentially obeys Gibrat's law in regime III.

Regimes I and II are observed when the product $\prod_{j=2}^T a_j$ tends to zero for large T and therefore z asymptotically approaches the absorbing state with $z = 0$. In this sense, regimes I and II define the absorbing phase of the model. Under this condition, $X_T \sim Z_T$, and therefore Z_T tends to a stationary random variable Z with $p(Z)$ given by the following equation (see a derivation in Sec. I of [47]):

$$p(Z) = \mathbb{E}_a \left[a^{-1} p \left(\frac{Z}{a} - 1 \right) \right]. \quad (3)$$

This can be reduced to a homogeneous Fredholm integral equation of the second kind [52] that is difficult to solve in general. We only solved it analytically for a specific case with $a \sim \mathcal{U}(0, c)$, which accurately matches the numerical results in region I, as shown in Fig. 2(b) [47] [see [45] for other exact solutions of Eq. (3)]. Even if Eq. (3) cannot be analytically solved in general, it is easy to show that regime I, where the first two moments of Z are finite, is observed for any distribution $f_a(a)$ provided $\mathbb{E}_a[a] = \bar{a} < 1$ and $\mathbb{E}_a[a^2] = v_a + \bar{a}^2 < 1$ [47] (Sec. II). The boundary between regimes I and II is then given by the condition $\mathbb{E}_a[a^2] = 1$, or equivalently $v_a = 1 - \bar{a}^2$ for any PDF $f_a(a)$.

To investigate the properties of regime II and its boundary with regime III, we insert a power-law tail ansatz, $p(Z) \propto Z^{-\alpha}$, into Eq. (3). From this we find that the exponent α is given by the zeros of the function

$$h(\alpha) = \mathbb{E}_a[a^{\alpha-1}] - 1. \quad (4)$$

The function $h(\alpha)$ has a root at $\alpha = 1$ due to the normalization of $f_a(a)$, which implies $\mathbb{E}_a[1] = 1$. However, we are only interested in roots with $\alpha \in (1, 3]$, irrespective of the specific form of $f_a(a)$. The condition $\alpha > 1$ ensures that $p(Z)$ is normalizable, and the condition $\alpha \leq 3$ corresponds to the boundary between regimes I and II where $\mathbb{E}_a[a^2] = 1$.

Figure 3 illustrates the behavior of $h(\alpha)$ for a uniformly distributed a with fixed v_a and various values of \bar{a} . A similar behavior is expected for any distribution $f_a(a)$ since $h(\alpha)$ is strictly convex for any $f_a(a)$ in the interval with $\alpha \geq 1$. Therefore, $h(\alpha)$ has at most one minimum and one root in

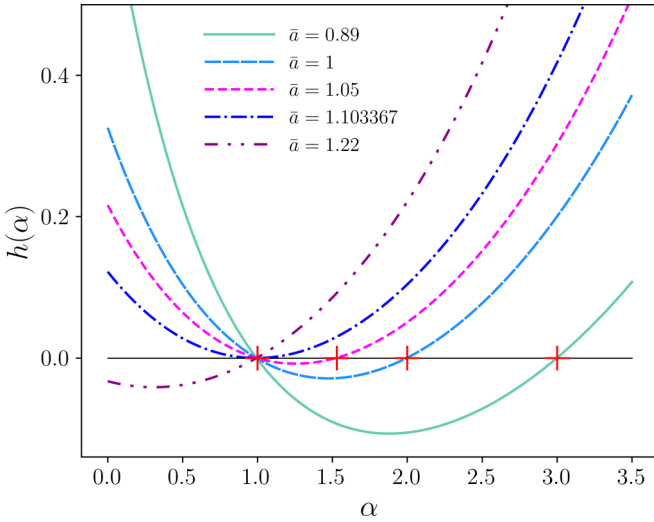


FIG. 3. Function $h(\alpha)$ [Eq. (4)] for a uniformly distributed reproduction rate (see Sec. III C of [47] for the exact analytic form). Different curves correspond to different values of \bar{a} for growth processes with $v_a = 0.2$. The exponent of the power-law tail for $p(Z)$ in regime II corresponds to the roots of $h(\alpha)$ in the interval of $\alpha \in (1, 3]$. This corresponds to curves with $0.89 \lesssim \bar{a} \lesssim 1.1$ in this example.

the interval of interest, (1,3]. As illustrated in Fig. 3, the root of $h(\alpha)$ decreases with increasing \bar{a} from the value $\alpha = 3$ at the boundary between regimes I and II to approach the minimum admissible value, $\alpha = 1$, which marks the transition from regime II to regime III. At the transition between regimes II and III, the minimum of $h(\alpha)$ occurs at $\alpha = 1$, and this leads to the condition

$$h'(1) = \mathbb{E}_a[\ln a] = 0 \tag{5}$$

for the boundary between the two regimes. The specific shape of the boundary in the space (\bar{a}, v_a) depends on the specific distribution of a . Equation (5) allows the relation between \bar{a} and v_a to be obtained for any $f_a(a)$. In particular, we obtained analytical results for uniformly and exponentially distributed a which compare well with numerical results (see Fig. 1 and more details in [47]).

In fact, the condition $\mathbb{E}_a[\ln a] = 0$ holds at the boundary between regimes with stationary and nonstationary $p(Z_T)$, irrespective of the power-law assumption made for regime II. Indeed, if $\mathbb{E}_a[\ln^2 a] < \infty$, the strong law of large numbers [42] allows us to express $\prod_{j=2}^T a_j$ as $e^{T\mathbb{E}_a[\ln a]}$ for large T . Accordingly, the sign of $\mathbb{E}_a[\ln a]$ determines whether $\prod_{j=2}^T a_j$ tends to zero and Z_T reaches a stationary regime (if $\mathbb{E}_a[\ln a] < 0$, regimes I and II) or increases for increasing T and Z_T is not stationary (if $\mathbb{E}_a[\ln a] > 0$, regime III). For a power-law $p(Z)$, one can see the change in sign of $\mathbb{E}_a[\ln a]$ at the transition between regimes II and III in terms of the slope $h'(1)$, which is negative in regime II and positive in regime III (see Fig. 3).

Conclusions. We showed that power-law [18,53] and log-normal avalanches can coexist in a minimal random growth

model with a reproduction rate with finite mean and variance. Interestingly, the power-law tail exponent α can be continuously tuned in the range (1,3] by varying the control parameters. Therefore, our study can explain several power laws found in natural or human processes, such as the ones described in [18], whose exponents are also almost always in the interval (1,3]. Many of these phenomena have an underlying multiplicative process and can be interpreted as avalanches. We have focused on growth processes with a finite value for \bar{a} and v_a . It is worth noting, however, that the condition determining a transition from a stationary distribution to a nonstationary one [Eq. (5)] and the definition of the exponent α [Eq. (4)] remain valid even if one (or both) of the parameters diverges (provided $\mathbb{E}_a[\ln^2 a] < \infty$). This is consistent with previous studies, where a power-law distributed growth rate was considered [54].

The model studied in this paper can be seen as a generalization of branching processes that correspond to a specific distribution for the growth rate (Sec. VII of [47]). In particular, the exponent $\alpha = 3/2$ observed for power-law distributed avalanche sizes in critical branching processes [32,33] is contained within the interval (1,3] obtained here. In addition to power-law and log-normal distributions, we observed, especially in the finite scale regime (but also along the upper bound of Fig. 1), less common distributions for avalanches, but nonetheless observed experimentally, such as the bimodal shape shown in Sec. III A of the supplemental material.

We assumed that \bar{a} and v_a remain constant during the course of the avalanches. One could, however, consider dynamical parameters to mimic feedback mechanisms, such as vaccination in epidemics or refractoriness in neuronal avalanches. In this case, our phase diagram in Fig. 1 can be used to propose qualitative scenarios for the ongoing controversy on log-normal or power-law distributions in neuroscience and other domains [21–23]. Indeed, besides giving an interpretation of the different distributions in terms of \bar{a} and v_a , it has to be seen as a guide for avalanche distributions, even for more realistic situations in which the control parameters are functions of time, as in [14,27,37,55]. This corresponds to a path in the diagram where the distributions are combined with different weights. For example, an avalanche with initial parameter values in region III, shifting in time toward region II or I (because of external feedbacks such as refractoriness in the brain), would give a log-normal dominating distribution. This qualitative scheme suggests that the three avalanche regimes identified here are relevant to realistically complex situations with nonstationary a_t . A more precise description of the avalanche size in such situations, however, would require extending our analysis to Gibrat’s processes with nonstationary a_t .

We thank J. P. Bouchaud for constructive comments. We acknowledge financial support from the Agence Nationale de la Recherche (ANR Grant No. ANR-18-CE45-0012-01) and from the French Research Ministry (MESR) (Contract No. 2017-SG-D-09) and from ENS Lyon for SP Ph.D. funding. F.J.P.R. acknowledges financial support from the Carnegie Trust.

- [1] C. J. Rhodes, H. J. Jensen, and R. M. Anderson, *Proc. R. Soc. London, Ser. B* **264**, 1639 (1997).
- [2] O. A. Pinto and M. A. Muñoz, *PLoS ONE* **6**, e21946 (2011).
- [3] F. Black and M. Scholes, *J. Polit. Econ.* **81**, 637 (1973).
- [4] J. M. Beggs and D. Plenz, *J. Neurosci.* **23**, 11167 (2003).
- [5] N. Friedman, S. Ito, B. A. W. Brinkman, M. Shimono, R. E. Lee DeVille, K. A. Dahmen, J. M. Beggs, and T. C. Butler, *Phys. Rev. Lett.* **108**, 208102 (2012).
- [6] J. A. Roberts, K. K. Iyer, S. Finnigan, S. Vanhatalo, and M. Breakspear, *J. Neurosci.* **34**, 6557 (2014).
- [7] B. Gutenberg and C. F. Richter, *Bull. Seismol. Soc. Am.* **32**, 163 (1942).
- [8] B. Gutenberg and C. F. Richter, *Bull. Seismol. Soc. Am.* **46**, 105 (1956).
- [9] F.-J. Pérez-Reche, M. Stipcich, E. Vives, L. Mañosa, A. Planes, and M. Morin, *Phys. Rev. B* **69**, 064101 (2004).
- [10] M. C. Gallardo, J. Manchado, F. J. Romero, J. del Cerro, E. K. H. Salje, A. Planes, E. Vives, R. Romero, and M. Stipcich, *Phys. Rev. B* **81**, 174102 (2010).
- [11] J. P. Sethna, K. Dahmen, S. Kartha, J. A. Krumhansl, B. W. Roberts, and J. D. Shore, *Phys. Rev. Lett.* **70**, 3347 (1993).
- [12] J. P. Sethna, K. A. Dahmen, and C. R. Myers, *Nature (London)* **410**, 242 (2001).
- [13] J. Baró, A. Corral, X. Illa, A. Planes, E. K. H. Salje, W. Schranz, D. E. Soto-Parra, and E. Vives, *Phys. Rev. Lett.* **110**, 088702 (2013).
- [14] S. Polizzi, B. Laperrousaz, F. Perez-Reche, F. Nicolini, V. Satta, A. Arneodo, and F. Argoul, *New J. Phys.* **20**, 053057 (2018).
- [15] L. Streppa, F. Ratti, E. Goillot, A. Devin, L. Schaeffer, A. Arneodo, and F. Argoul, *Sci. Rep.* **8**, 1 (2018).
- [16] C. Kleiber and S. Kotz, *Statistical Size Distributions in Economics and Actuarial Sciences*, Wiley Series in Probability and Statistics (Wiley, Hoboken, NJ, 2003).
- [17] D. Sornette, *Critical Phenomena in Natural Sciences: Chaos, Fractals, Self-Organization and Disorder: Concepts and Tools* (Springer Science & Business Media, New York, 2006).
- [18] M. E. Newman, *Contemp. Phys.* **46**, 323 (2005).
- [19] M. P. H. Stumpf and M. A. Porter, *Science* **335**, 665 (2012).
- [20] A. Clauset, C. R. Shalizi, and M. E. Newman, *SIAM Rev.* **51**, 661 (2009).
- [21] J. M. Beggs and N. Timme, *Front. Phys.* **3**, 163 (2012).
- [22] G. Buzsáki and K. Mizuseki, *Nat. Rev. Neurosci.* **15**, 264 (2014).
- [23] A. D. Broido and A. Clauset, *Nat. Commun.* **10**, 1 (2019).
- [24] E. W. Montroll and M. F. Shlesinger, *Proc. Natl. Acad. Sci. USA* **79**, 3380 (1982).
- [25] A. P. Mehta, A. C. Mills, K. A. Dahmen, and J. P. Sethna, *Phys. Rev. E* **65**, 046139 (2002).
- [26] F. J. Pérez-Reche and E. Vives, *Phys. Rev. B* **67**, 134421 (2003).
- [27] F.-J. Pérez-Reche, C. Triguero, G. Zanzotto, and L. Truskinovsky, *Phys. Rev. B* **94**, 144102 (2016).
- [28] H. Borja da Rocha and L. Truskinovsky, *Phys. Rev. Lett.* **124**, 015501 (2020).
- [29] P. Bak, *How Nature Works: The Science of Self-Organized Criticality* (Springer Science & Business Media, New York, 2013).
- [30] F. Pázmándi, G. Zaránd, and G. T. Zimányi, *Phys. Rev. Lett.* **83**, 1034 (1999).
- [31] G. U. Yule, *Philos. Trans. R. Soc. London, Ser. B* **213**, 21 (1925).
- [32] T. E. Harris, *The Theory of Branching Processes, Dover Phoenix Editions* (Springer-Verlag, Berlin, 1963).
- [33] A. Corral and F. Font-Clos, in *Self-organized Criticality Systems* (Open Academy, Berlin, 2013), Chap. 5, pp. 183–228.
- [34] J. P. Gleeson and R. Durrett, *Nat. Commun.* **8**, 1227 (2017).
- [35] S. di Santo, P. Villegas, R. Burioni, and M. A. Muñoz, *Phys. Rev. E* **95**, 032115 (2017).
- [36] S. Zapperi, K. B. Lauritsen, and H. E. Stanley, *Phys. Rev. Lett.* **75**, 4071 (1995).
- [37] T. P. Handford, F. J. Pérez-Reche, and S. N. Taraskin, *Phys. Rev. E* **87**, 062122 (2013).
- [38] R. Gibrat, *Bull. Stat. Gén. France* **19**, 469 (1930).
- [39] R. Gibrat, *Les Inégalités Economiques* (Librairie du Recueil Sirey, Paris, 1931).
- [40] J. M. Sancho, M. San Miguel, S. L. Katz, and J. D. Gunton, *Phys. Rev. A* **26**, 1589 (1982).
- [41] S. Redner, *Am. J. Phys.* **58**, 267 (1990).
- [42] G. Grimmett and D. Stirzaker, *Probability and Random Processes*, 3rd ed. (Oxford University Press, Oxford, 2001).
- [43] H. Kesten, *Acta Math.* **131**, 207 (1973).
- [44] C. M. Goldie, *Ann. Appl. Prob.* **1**, 126 (1991).
- [45] C. de Calan, J. M. Luck, T. M. Nieuwenhuizen, and D. Petritis, *J. Phys. A* **18**, 501 (1985).
- [46] T. Gautié, J.-P. Bouchaud, and P. L. Doussal, *J. Phys. A* **54**, 255201 (2021).
- [47] See Supplemental Material at <http://link.aps.org/supplemental/10.1103/PhysRevE.104.L052101> for more details on numerical results on the described regimes (for uniformly and exponentially distributed growth rates) and on analytical calculations and statistical methods, which includes additional Refs. [S3,S4].
- [48] V. Da Costa, Y. Henry, F. Bardou, M. Romeo, and K. Ounadjela, *Eur. Phys. J. B* **13**, 297 (2000).
- [49] H. Mouri, *Phys. Rev. E* **88**, 042124 (2013).
- [50] J. Alstott, E. Bullmore, and D. Plenz, *PLoS ONE* **9**, e85777 (2014).
- [51] A. C. Davison and D. V. Hinkley, *Bootstrap Methods and their Application* (Cambridge University Press, New York, 1997), Chap. 2.
- [52] W. H. Press, S. A. Teukolsky, W. T. Vetterling, and B. P. Flannery, *Numerical Recipes*, 3rd ed. (Cambridge University Press, Cambridge, UK, 2007).
- [53] H. Takayasu, A.-H. Sato, and M. Takayasu, *Phys. Rev. Lett.* **79**, 966 (1997).
- [54] A. Saichev, A. Helmstetter, and D. Sornette, *Pure Appl. Geophys.* **162**, 1113 (2005).
- [55] S. Polizzi, A. Arneodo, F.-J. Pérez-Reche, and F. Argoul, *Front. Appl. Math. Stat.* **6**, 73 (2021).